HIAPER Cloud Radar (HCR) data (CfRadial), Version 1.1

Changes from Version 1.0

LDR censoring in regions with low signal to noise ratio has been improved.

New experimental fields were added and we welcome feedback on their performance:

An echo type classification algorithm ECCO-V (Echo Classification from COnvectivity - Vertical pointing) was developed and applied. It adds a 2D (time, range) CONVECTIVITY field, which provides a quantitative measure of how convective each gridpoint is, with 0 indicating all stratiform and 1 indicating all convective echo. CONVECTIVITY is then translated into a 2D convective/stratiform partitioning field ECHO_TYPE_2D which provides several convective/stratiform echo classifications. The 2D field is composited into a 1D (time) ECHO_TYPE_1D field. Details can be found in Romatschke and Dixon (2022).

Particle IDentification (PID) was added with a newly developed algorithm which is based on a fuzzy logic scheme. It identifies different sizes of particles and in some cases provides particle phase (liquid/frozen). Details can be found in Romatschke and Vivekanandan (2022).

Overview

This dataset contains HIAPER Cloud Radar (HCR) data collected aboard the NSF/NCAR GV HIAPER (Gulfstream-V High-performance Instrumented Airborne Platform for Environmental Research, HIAPER) (N677F) aircraft during SPICULE (Secondary Production of Ice in Cumulus Experiment). The data were collected during 10 research flights which took place between May 29 and June 25, 2021, over the US Great Plains. For more information on SPICULE, see https://www.eol.ucar.edu/field_projects/spicule.

Flight	Start date	Start time UTC	End date	End time UTC
RF01	2021 05 29	15:15	2021 05 29	19:56
RF02	2021 06 01	16:45	2021 06 01	21:18
RF03	2021 06 02	20:40	2021 06 03	01:23
RF04	2021 06 05	13:46	2021 06 05	21:59
RF05	2021 06 09	19:50	2021 06 09	23:34
RF06	2021 06 11	17:45	2021 06 12	00:03
RF07	2021 06 17	18:20	2021 06 18	00:44
RF08	2021 06 20	18:50	2021 06 21	04:00
RF09	2021 06 24	19:55	2021 06 24	23:46
RF10	2021 06 25	18:45	2021 06 25	22:49

Instrument description

HCR is an airborne, polarimetric, millimeter-wavelength (W-band) radar that serves the atmospheric science community by providing cloud remote sensing capabilities to the NSF/NCAR G-V (HIAPER) aircraft. HCR detects ice and liquid clouds and collects Doppler radial velocity measurements, which at vertical incident is dominated by the vertical particle fall speed.

In a pod-based design, a single lens antenna is used for both transmit and receive. The transceiver uses a two-stage up and down conversion superheterodyne design. The transmit waveform, from a waveform generator, passes through the two-stage up-conversion to the transmit frequency of 94.40625 GHz. It is then amplified by an extended interaction klystron amplifier (EIKA) to 1.6 kW peak power. System performance on transmit and receive paths are closely monitored using a coupler and a noise source. Raw in-phase and quadrature information are archived. For more information, see Vivekanandan et al. (2015) and www.eol.ucar.edu/instruments/hiaper-cloud-radar-hcr

HIAPER Cloud Radar Specifications	
Parameter	**Specification**
Antenna	0.3 m, lens
Antenna gain	46.21 dB
Antenna 3 dB beam width	0.72°
Transmit Polarization	Linear (V)
Transmit frequency	94.40625 GHz
Transmitter	Klystron
Peak transmit power	1.6 kW
Pulse width	0.2 – 1.0 μs
PRF	10 kHz
System noise power	-101 dBm
Receiver noise figure	8.9 dB
Receiver Bandwidth	20 MHz
Receiver Dynamic Range	76 dB
First IF	156.25 MHz
Second IF	1406.25

Range resolution	19.2 m, 38.4 m
Unambiguous range	15 km
Along-flight track resolution	60 m
Typical reflectivity uncertainty	0.4 dB
Sensitivity	-31.5 dBZ at 1 km
Unambiguous velocity	±7.83 m/s
Typical radial velocity uncertainty	0.2 m/s at W=2 m/s
Dwell time	100 ms

Data description

The 10 Hz moments data described here are available at http://data.eol.ucar.edu/dataset/605.011. in CfRadial format. For more information on CfRadial see www.ral.ucar.edu/projects/titan/docs/radial_formats/CfRadialDoc.pdf.

The primary data products for scientific use are listed in the table below.

Variable	Dimensions	Unit	Long Name
time	time	seconds	Time in seconds since volume start
	time	meters	Range from instrument to center of gate
latitude	time	deg	Latitude
longitude	time	deg	Longitude
altitude	time	m	Altitude of radar
DBZ	time, range	dBZ	Reflectivity
DBZ_MASKED	time, range	dBZ	Reflectivity of cloud echo only (DBZ(FLAG>1)=NAN, see FLAG below)
VEL_UNFOLDED	time, range	m/s	Motion and bias corrected, and de-aliased Doppler velocity
VEL_MASKED	time. range	m/s	VEL_UNFOLDED but for vertical pointing time periods only (ANTFLAG equals 1 or 2, see below)
WIDTH	time, range	m/s	Spectral width
SNR	time, range	dB	Signal to noise ratio
DBMVC	time, range	dBm	Log power co-polar v transmit, v receive
DBMHX	time, range	dBm	Log power cross-polar v transmit, h receive
NCP	time, range		Normalized coherent power
LDR	time, range	dB	Linear depolarization ratio (V/H)
LDR_MAKSED	time, range	dB	Linear depolarization ratio (V/H) of cloud only data corrected for

			H-channel issue (see below)
PRESS	time, range	hPa	Air pressure from ERA5
TEMP	time, range	C	Air temperature from ERA5
RH	time, range	%	Relative humidity from ERA5
U_SURF	time	m/s	Surface U wind component from ERA5 forecast
V_SURF	time	m/s	Surface V wind component from ERA5 forecast
TOPO	time	m	Terrain elevation above mean sea level from GTOPO30 (U.S. Geological Survey, 2019)
FLAG	time, range		See Romatschke et al. (2021) Flag field to classify reflectivity (to mask unwanted data): 1 Cloud 2 Speckle (contiguous 2D echo areas of < 100 pixels) 3 Extinct (signal completely attenuated) 4 Backlobe echo (reflection from the land/sea surface when zenith pointing and flying low) 5 Out of range (second trip echo from land/sea surface when flying too high) 6 Transmitter pulse (echo from within the radar itself) 7 Water surface echo 8 Land surface echo 9 Below the surface 10 Noise source calibration 11 Missing (not transmitting)
ANTFLAG	time		Flag field to indicate the status of the antenna: 1 Down (nadir pointing) 2 Up (zenith pointing) 3 Pointing (pointing to an angle different from nadir or zenith) 4 Scanning (e.g. sea surface calibration) 5 Transition (e.g. from nadir to zenith) 6 Failure
MELTING_LAYER	time, range		See Romatschke (2021) 10 below icing level 11 ERA5 0 °C isotherm below icing level 12 detected melting layer below or at icing level 13 interpolated melting layer below or at icing level 14 estimated melting layer below or at icing level 20 above icing level 21 ERA5 0 °C isotherm above icing level 22 detected melting layer above icing level 23 interpolated melting layer above icing level 24 estimated melting layer above icing level

ICING_LEVEL	time	m	Altitude of icing level, which is defined as the lowest melting layer
ECHO_TYPE_2D	time, range		See Romatschke and Dixon (2022) 14 stratiform low 16 stratiform mid 18 stratiform high 25 mixed 30 convective 32 convective elevated 34 convective shallow 36 convective mid 38 convective deep
ECHO_TYPE_1D	time		As ECHO_TYPE_2D
PID	time, range		See Romatschke and Vivekanandan (2022) 1 rain 2 supercooled rain 3 drizzle 4 supercooled drizzle 5 cloud liquid 6 supercooled cloud liquid 7 melting 8 large frozen 9 small frozen 10 precipitation 11 cloud

Data processing and quality control

A detailed description of the data processing and quality control procedures can be found in Romatschke et al. (2021).

Power fields (DBZ, DBZ_MASKED, DBMVC, DBMHX)

As an external, pod-mounted system, which is deployed in a wide range of altitudes from near surface to approximately 15 km, HCR experiences large temperature variations. To maintain good system calibration, it is essential to monitor the radar system performance versus temperature. In order to ensure operational accuracy, a number of noise source calibration (NScal) events were performed during SPICULE research flights, and on the ground. During each NScal event, a known noise signal, which is invariant to temperature changes, is injected into the radar and then used to characterize the receiver gain changes by comparing the received power (DBMVC) to a temperature-corrected noise power.

Correlation equations gained from the NScal events were used (together with the calibration data obtained in the lab) to correct the power fields (DBMVC, DBMHX, and DBZ) for temperature changes in the whole data set (Romatschke et al., 2021).
The FLAG field (Romatschke et al., 2021) is used to mask out all non-cloud data in the DBZ_MASKED field.

Radial velocity (VEL, VEL_CORR, VEL_UNFOLDED, VEL_MASKED)

The radial velocity is corrected for platform motion using two different methods. The first corrects for platform motion using INS/GPS measurements. It is applied to all of the data in the VEL field. An additional correction is applied to the nadir-looking data only: The radial velocity of the surface, which is assumed to be 0 m/s, is used as a reference to correct the data with a running 3rd degree polynomial filter of length 15 seconds (Ellis et al., 2019, Romatschke et al., 2021). This second correction is reflected in the VEL_CORR field.

During SPICULE strong up and down drafts were sampled. Since the nyquist velocity of HCR is ~7.8 m/s a de-aliasing algorithm was developed to unfold VEL_CORR resulting in the VEL_UNFOLDED field. The de-aliasing algorithm is only applied to cloud data (as determined by the FLAG field) and therefore VEL_UNFOLDED only contains cloud data (similar to DBZ_MASKED).

Generally, the rotatable reflector design of the HCR antenna allows for beam stabilization for changes in roll and pitch angles due to platform motion in real time. However, in some situations the antenna steering cannot adjust for platform motions because of hardware limitations in the steering mechanism. The most noticeable instances are during steep climbs and in right turns of the aircraft in zenith pointing mode. In these cases the antenna will not point directly at zenith or nadir and therefore VEL_UNFOLDED cannot be interpreted as vertical velocity. We created a VEL_MASKED field which only contains vertical pointing data as determined by the ANTFLAG field values 1 and 2.

WIDTH correction

The radar has a 0.73° beam width. Therefore, when pointing nadir or zenith, the beam spread is about 0.36° forward of the vertical, and 0.36° aft of the vertical. The sine of 0.36° is 0.006, so at a ground speed of 200 m/s the velocity error at the forward edge of the beam is -0.006 x 200 = -1.2 m/s, since the motion is towards the radar. Similarly the velocity error at the aft edge of the beam is +1.2 m/s. These errors, across the width of the beam, increase the variance of the measured velocity, and hence increase the spectrum width. The computed width correction (delta below) is based on ground speed and beam width, and attempts to correct for this increase.

$$\delta = |(0.3 * speed * sin(elevation) * beamWidthRadians)|$$

$$corrected = \sqrt{(measured^2 - \delta^2)}$$

Known problems

H-channel problem

Starting in RF5 HCR experienced problems in the H-channel (the cross-polar channel) which manifested as an increase in the noise floor and stripes in the H fields. The problem occurred intermittently throughout the rest of the project. The main variables affected are DBMHX and LDR. We developed a method to greatly reduce the effects in LDR that is applied to create the LDR_MASKED field (which shows only cloud data, as do the other MASKED fields) but caution is still advisable. Fortunately the problem occurred mostly during clear air periods and only very few cloudy times were affected. The most serious example is shown below.

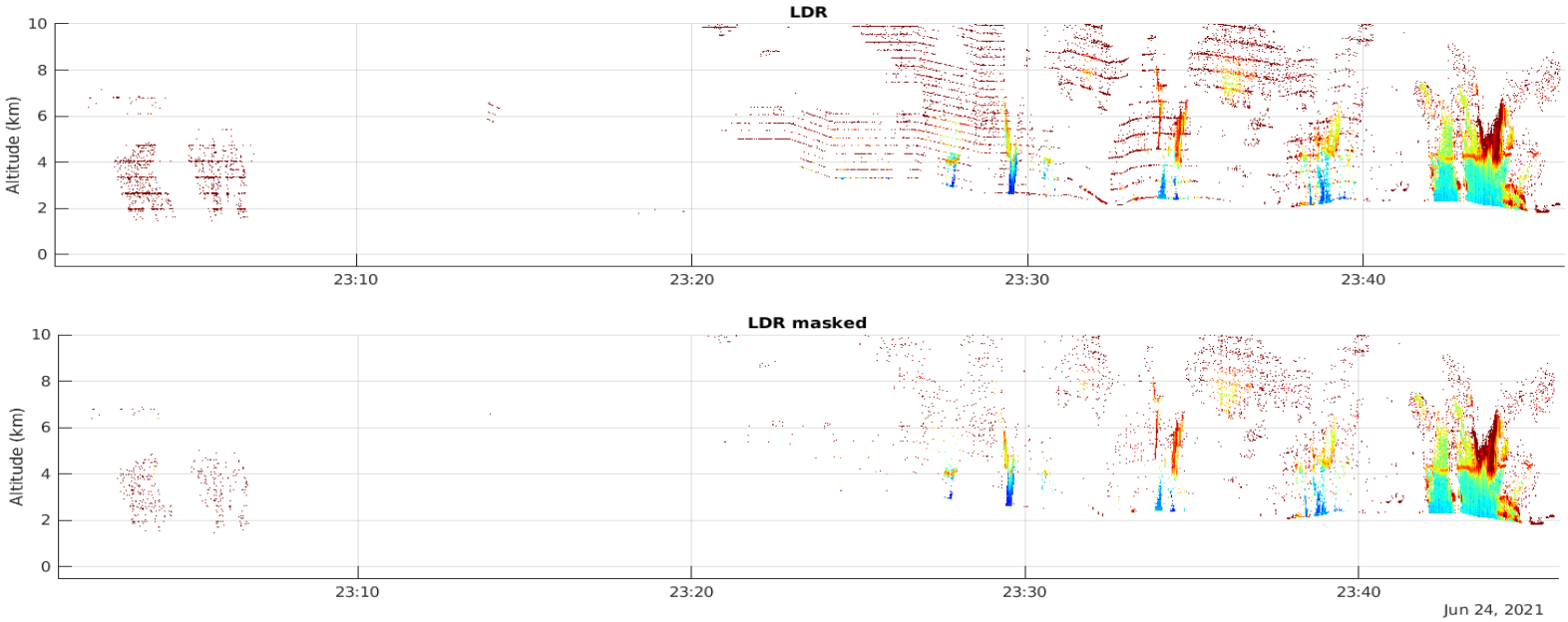

Multiple scattering

In areas of heavy convection HCR data is affected by multiple scattering. Affected areas show increased LDR as seen in the example below. Reflectivity in these areas is likely not accurate and should be used with caution. PID is likely also not correct. We are currently investigating the multiple scattering problem and hope to have more information in the future.

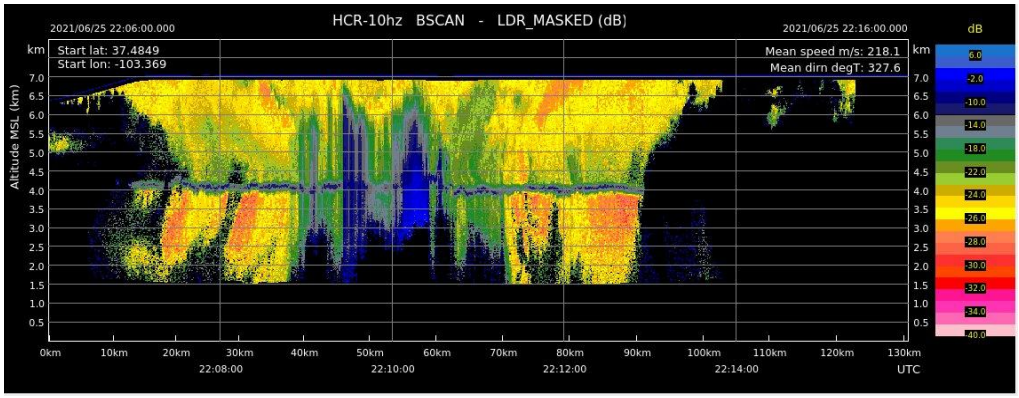

Back-lobe echo in zenith pointing

When the HCR is pointing at zenith and the GV is near the surface, there is often an echo that results from the back-lobe of the radar reflecting off of the surface. This back-lobe contamination is typically characterized by a band of low reflectivity, highly variable radial velocity, and high spectrum width. The back-lobe appears in the zenith data at a range equal to the altitude of the radar. So as the GV ascends or descends the back-lobe contamination will recede and approach in range, respectively. An attempt was made to identify the back-lobe echo and flag it in the FLAG field but the identification process does not always completely remove all back-lobe echo but in rare cases removes cloud data. Both of these effects can be seen in the example below. We are currently exploring options to mitigate this problem.

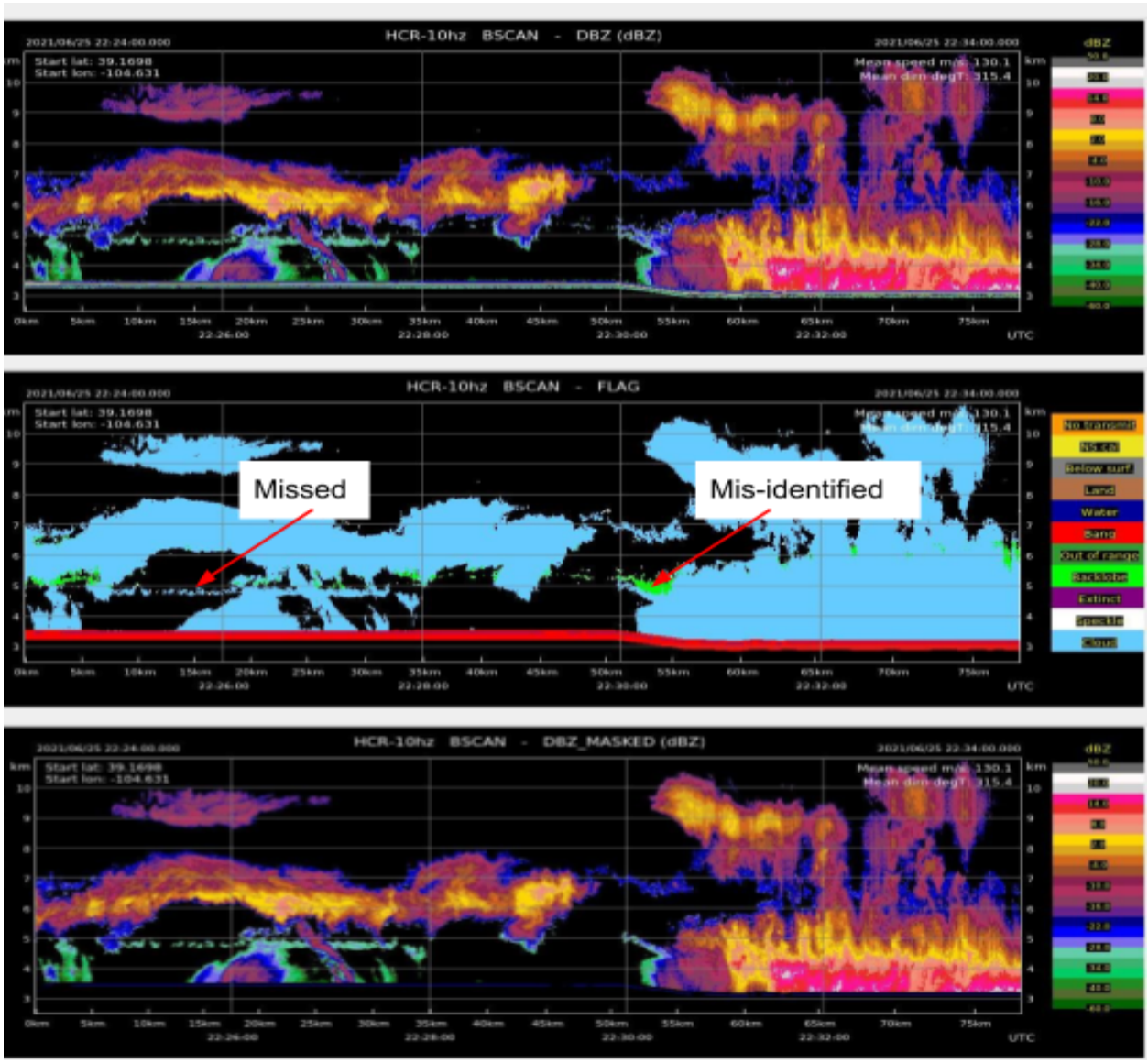

Melting layer detection

In the early stages of the life cycle of convective clouds, such as those observed during SPICULE, the melting layer is often not yet fully developed which sometimes causes problems for the HCR melting layer detection algorithm (Romatschke, 2021). Therefore, some melting layer signatures are missed and in rare cases the melting layer is detected at the wrong altitude.

References

Ellis, S.M., P. Tsai, C. Burghart, U. Romatschke, M. Dixon, J. Vivekanandan, J. Emmett, and E. Loew, 2019: Use of the Earth's Surface as a Reference to Correct Airborne Nadir-Looking Radar Radial Velocity Measurements for Platform Motion. J. Atmos. Oceanic Technol., 36, 1343–1360, https://doi.org/10.1175/JTECH-D-19-0019.1.

Romatschke, U., M. Dixon, P. Tsai, E. Loew, J. Vivekanandan, J. Emmett, R. Rilling, 2021: The NCAR Airborne 94-GHz Cloud Radar: Calibration and Data Processing. Data, 6, 66. https://doi.org/10.3390/data6060066.

Romatschke U., 2021: Melting Layer Detection and Observation with the NCAR Airborne W-Band Radar. Remote Sensing. 13(9):1660. https://doi.org/10.3390/rs13091660.

Romatschke, U., Vivekanandan, V., 2022: Cloud and Precipitation Particle Identification Using Cloud Radar and Lidar Measurements: Retrieval Technique and Validation. Earth and Space Science Open Archive, https://doi.org/10.1002/essoar.10510625.1.

Romatschke, U., Dixon, M., 2022: Vertically Resolved Convective/StratiformEcho Type Identification and ConvectivityRetrieval for Vertically Pointing Radars. EarthArXiv, https://doi.org/10.31223/X54S77.

Vivekanandan, J., Ellis, S., Tsai, P., Loew, E., Lee, W.-C., Emmett, J., Dixon, M., Burghart, C., and Rauenbuehler, S., 2015: A wing pod-based millimeter wavelength airborne cloud radar, Geosci. Instrum. Method. Data Syst., 4, 161-176, https://doi.org/10.5194/gi-4-161-2015

Data citation

NCAR/EOL Remote Sensing Facility. 2022. SPICULE: NCAR HCR radar moments data. Version 1.1. UCAR/NCAR - Earth Observing Laboratory. https://doi.org/10.26023/PGGK-MC4T-K70F. Accessed <YYYY-MM-DD>.

Contact

EOL Data Support: eol-datahelp@ucar.edu

UCAR/NCAR - Earth Observing Laboratory
Remote Sensing Facility
HIAPER Cloud Radar
http://doi.org/10.5065/D6BP00TP